ISSN 1064-2269, Journal of Communications Technology and Electronics, 2017, Vol. 62, No. 8, pp. 886–893. © Pleiades Publishing, Inc., 2017.
Original Russian Text © L.N. Anishchenko, A.S. Bugaev, S.I. Ivashov, A.B. Tataraidze, M.V. Bochkarev, L.S. Korostovtseva, Yu.V. Sviryaev, 2017, published in Radiotekhnika i Elektronika, 2017, Vol. 62, No. 8, pp. 787–794.

APPLICATIONS OF RADIOTECHNOLOGY AND ELECTRONICS IN BIOLOGY AND MEDICINE

Determination of the Sleep Structure via Radar Monitoring of Respiratory Movements and Motor Activity

L. N. Anishchenko[a], A. S. Bugaev[a, c], S. I. Ivashov[a], A. B. Tataraidze[a, *], M. V. Bochkarev[b], L. S. Korostovtseva[b], and Yu. V. Sviryaev[b]

[a] *Bauman State Technical University (National Research University), Moscow, 105005 Russia*
[b] *Almazov North-West Federal Medical Research Center, Ministry of Healthcare of the Russian Federation, St. Petersburg, 197341 Russia*
[c] *Moscow Institute of Physics and Technology (State University), Dolgoprudnyi, Moscow oblast, 141700 Russia*
**e-mail: tataraidze@rslab.ru*

Received March 13, 2017

Abstract—The issue of long-term automatic determination of the human sleep structure through the analysis of respiratory movements and motor activity recorded using bioradiolocation is considered. An algorithm for the determination of the human sleep structure is developed. The potentiality of determining the sleep structure with an average quality of 0.5 Cohen's kappa relative to the "gold standard" (polysomnography) for apparently both healthy test subjects and insomniacs is demonstrated.

DOI: 10.1134/S1064226917080022

INTRODUCTION

Sleep disorders are common among humans and are often left undiagnosed. In the near term outlook, these disorders lead to a marked deterioration of the quality of life; in the long term outlook, they raise the risk of cardiovascular diseases, obesity, pancreatic diabetes, mental disorders, and premature death.

The sleep structure is the key measurable indicator in diagnosing of insomnia and other sleep disorders. Polysomnography (PSG) is the "gold standard" of determination of the sleep structure. The PSG is a method of long-term monitoring of physiological parameters during sleep. Analyzing the PSG results (electroencephalogram, electrooculogram, and electromyogram) visually, a physician classifies each epoch (30-second recording interval) as a wakefulness period (WP), a rapid eye movement sleep (REMS), or one of the three stages of a slow sleep or a non-rapid eye movement sleep (NREMS) . The first and the second NREMS stages are often combined into one (light sleep, LS), and the third stage is called a deep sleep (DS).

The following methods are currently used in the clinical practice for evaluation of the sleep–wake cycle and the sleep structure: the sleep diary, the PSG, and the actigraphy. The actigraphy is a method for distinguishing between sleep and wakefulness based on the analysis of motor activity of the nondominant hand. This activity is normally recorded with an accelerometer embedded into a bracelet. The actigraphy does not allow one to determine the sleep structure. The sleep diary method is subjective; it is based entirely on the information provided by the tested subject, who should be highly motivated to keep regular records. The polysomnography is costly and time-consuming, which limits its use. In addition, the tested subject feels discomfort during the test, and the sleep structure may thus be affected. This is especially important for insomniacs, since their processes of sleep initiation and maintenance are already disturbed.

Thus, new instrumental procedures for monitoring the sleep structure over extended time periods are needed. Such methods may be used to diagnose insomnia, detect sleep disorders at their early stages, monitor the efficiency of therapy, help tested subjects in control of the sleep–wake regime, attract their attention to their health, and motivate them to maintain sleep hygiene.

Noncontact methods for sleep monitoring, which cause the least discomfort, are of particular interest. One such method is bioradar (BR) monitoring of respiratory movements and motor activity of the tested subject. Bioradar is a technique for remote detection and diagnosing of biological objects based on the modulation of the radar signal by the oscillatory motion and displacement of organs [1].

Changes in the respiratory pattern during sleep occur due to weakening or lack of certain input stimuli that act on the respiratory center during waking hours; fluctuations in the autonomic regulation during sleep; atony of skeletal muscles during the REMS; an increase in the resistance of upper respiratory airway;

a reduction in the metabolic rate; and a reduction in the sensitivity of chemoreceptors [2]. The respiratory pattern is a combination of volume–temporal parameters of the respiratory cycle [3]. The potentiality of determining the sleep structure through the analysis of respiratory movements detected using respiratory inductance plethysmography (RIP), which is a common contact method included into the PSG, was demonstrated in [4].

The aim of this study is to develop an algorithm for classification of the sleep epochs (i.e, establishing of the correspondence between each epoch and one of the following classes: WP, REMS, LS, or DS) through the analysis of respiratory movements and motor activity of the tested subject that are recorded in the process of BR monitoring. This study is a continuation of our earlier research into the sleep structure [5–7].

1. MATERIALS AND TECHNIQUES

A. Experimental Data

Experiments on simultaneous recording of the BR and PSG signals were conducted in order to create a clinically verified database of BR signals from nocturnal sleep monitoring. This research was managed by the somnology working group at the Department of Arterial Hypertension (Almazov North-West Federal Medical Research Center). A total of 32 tested volunteers were involved in the study. In all 32 cases, the obtained results revealed no respiratory malfunctions or motor disturbances during sleep. Parameters of the BR sample are listed below:

Number of epochs	33964
Men : women	12 : 20
With insomnia : without insomnia	4 : 28
Age (years)	44.22 ± 15.44 (17.00...48.00)
Wakefulness, %	22.66 ± 12.53 (5.59...52.94)
REMS, %	18.15 ± 6.09 (9.31...34.04)
Light sleep, %	41.48 ± 7.99 (21.33...56.95)
Deep sleep, %	17.71 ± 5.93 (7.76...33.38)
Sleep efficiency, %	77.34 ± 12.53 (47.06...94.41)

Here, the mean value and the ± standard deviation are indicated. The range of variation is given in parentheses.

The PSG studies were conducted using an Embla N7000 (Natus Neurology Inc.) polysomnography system. Each epoch was classified by a physician from the results of visual analysis of the EEG, EOG, and EMG signals in accordance with the guidelines of the American Academy of Sleep Medicine. The obtained results of classification of sleep epochs wwere used as a set of true answers in the process of training and testing of the algorithm.

Fig. 1. Simultaneous PSG and BR monitoring.

The BR monitoring was performed in parallel with the PSG (Fig. 1) using a BioRaskan BR system designed at the Remote Sensing Laboratory (Bauman State Technical University). The BioRaskan is a bioradar that uses a continuous signal with stepped frequency modulation and a quadrature detector. It has eight operating frequencies in the range 3.6–4.0 GHz. The energy flux density (EFD) is 1.36 μW/cm^2, and the radiated power is no higher than 3 mW.

The total of 1636 PSG recordings from tested subjects without respiratory malfunctions during sleep (apnea–hypopnea index ≤5 event/h) from the open Sleep Heart Health Study (SHHS) database were used to develop a model for estimating the a priori probabilities of epochs belonging to certain classes [8–10]. The parameters of the SHHS sample are listed below:

Number of epochs	1760763
Men : women	404 : 1232
Men : women	60.77 ± 11.51 (39–90)
Age, years	60.77 ± 11.51 (39–90)
Wakefulness, %	29.38 ± 12.42 (2.62–82.99)
REMS, %	14.58 ± 5.90 (0–35.73)
Light sleep, %	42.31 ± 11.92 (6.48–93.64)
Deep sleep, %	13.73 ± 8.83 (0–51.38)
Sleep efficiency, %	76.19 ± 17.27 (36.54–99.05)

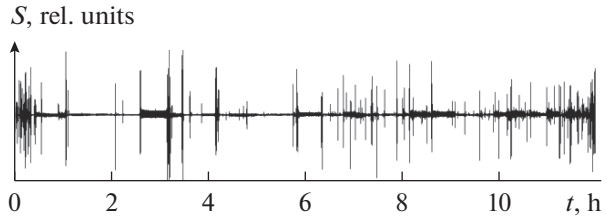

Fig. 2. The BR signal (S) before processing.

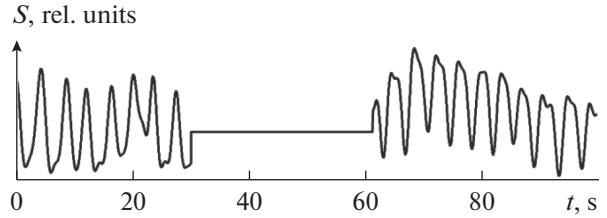

Fig. 3. The BR signal (S) during processing. The signal is oriented normally in the left part of the figure and is inverted in the right part. A suppressed artifact interval is seen at the center.

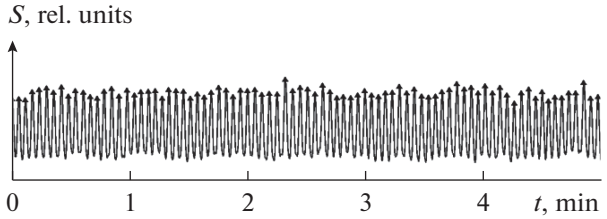

Fig. 4. Identification of respiratory cycles (marked with triangles) in the BR signal.

Here, the mean value and the ± standard deviation are indicated. The range of variation is given in parentheses.

B. Preprocessing of the BR Signal

Each BR recording contains 16 signals (eight operating frequencies with I and Q quadratures) recorded simultaneously. The quality of every signal may vary due to motion the tested subject (i.e., changes in the distance between the bioradar and the tested subject). The algorithm for preprocessing of the BR signal consists of the following stages: filtering, identification of artifacts, integration of interartifact intervals (IAIs), normalization of the IAI, orientation of the IAI correction, and identification respiratory cycles (RCs). Figure 2 shows the unprocessed BR signal.

The BR signals were filtered using a fifth-order bandpass Butterworth filter with cutoff frequencies of 0.05 and 0.6 Hz. The sampling rate of the BR signal was lowered from 50 to 10 Hz.

BR and PSG recordings were synchronized by means of peak-to-peak synchronization of the RIP and BR signals. The BR recordings were then cut at the onset of the first epoch identified by a physician and at the end of the last one.

Artifacts were identified in the BR signal with the maximum energy using a sliding window with a length of 15 s and a step of 1 s. Signal energy E_w was calculated for each window. The presence of an artifact within a window was established by comparing E_w with the threshold value of $0.7\overline{E_w}$, which was calculated using the signal energy averaged over the entire recording ($\overline{E_w}$.). The signal interval covering the entire window with an identified artifact and 2.5 s after this window was regarded as an artifact signal. If the distance between artifact intervals was shorter than 20 s, this signal interval was also regarded as an artifact signal.

Combined signal $S = \{IAI_1, AI_1, IAI_2, AI_2, \ldots IAI_n\}$, where AI is the artifact interval, was used in the subsequent analysis. Each IAI was replaced by the corresponding interval of the BR signal having the maximum energy in this IAI.

The signal within an IAI may be inverted (Fig. 3) due to the phase shift of the signal reflected from the biological object. This phase shift is caused by a change in the mean distance between the radar and the target resulted from the motor activity of the tested subject. The signal orientation with the peak between the inspiratory and expiratory RC phases pointing upwards was regarded as the normal orientation. Inversion of the IAI was identified by analyzing the average RC width and was corrected by flipping the inverted IAI.

The IAIs were normalized using Z-normalization. The RCs were identified by means of the search for the local maximum points in the IAIs. Figure 4 presents the results of RC identification. Each RC was characterized by the following parameters (Fig. 5): coordinates of the RC starting point (b_x, b_y); coordinates of the end point of the inspiratory phase (p_x, p_y); coordinates of the RC end point (e_x, e_y); the RC amplitude $A = p_y - \min(b_y, e_y)$; and the RC width $W = e_x - b_x$.

C. Extraction of Features

A set of features was assigned to each epoch. These features were extracted both directly from the target epoch and from the sliding windows with widths of 5, 11, and 25 epochs.

The following features were extracted from each epoch of signal S: the respiration rate evaluated in the spectral domain, the duration of the motor activity, the signal energy during the motor activity, the median of W, the standardized median of p_y, the standard deviation of W, the interquartile range of A, and the regu-

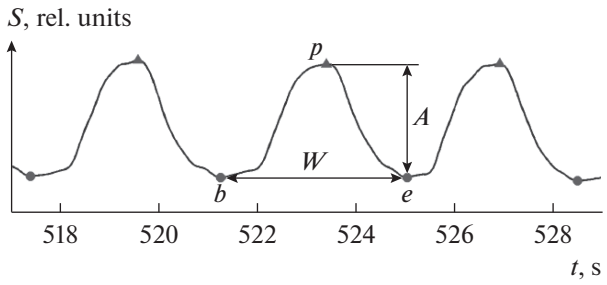

Fig. 5. Respiratory cycles in the BR signal: b is the RC starting point, p is the point of transition between inspiratory and expiratory RC phases, e is the RC end point, and A and W are the amplitude and width of the RC.

larity of the respiratory pattern evaluated using the sample entropy method.

The following features were extracted using the sliding window with a width of five epochs: the similarity between the respiratory pattern of the epoch and the patterns of neighboring epochs, which was evaluated using dynamic time wrapping [11], and the breath-by-breath correlation [12].

The standard deviation of the respiration rate [11] was extracted using the sliding window with a width of 11 epochs.

The following features mentioned in [4] were extracted using the sliding window with a width of 25 epochs: the median of A, the standardized median of p_y, the standardized median of b_y, the "expiratory flow rate", the entropy of the p_y sample, the "flow rate", the "inspiratory flow rate", the standardized median of the "respiratory volume" in the expiratory phase, the entropy of the b_y sample, and the standardized median of the "respiratory volume."

In order to reduce the cross-individual variability of values of the extracted features, Z-normalization of each feature extracted from a BR signal was performed for each recording. In addition, a standardized epoch number (an integer falling within the range of 1–100) was assigned to each epoch.

D. Classification of Epochs

Classification of epochs involved five stages (Fig. 6): the primary classification, the secondary classification, splitting the recording into sleep cycles, estimation of a priori probabilities, and the final classification.

The primary classification was performed using the gradient tree boosting with solutions from the XGBoost library [13]. The probabilities of an epoch belonging to a certain class were estimated at this stage.

These probabilities for the target epoch and six neighboring epochs on each side of it were used as the feature vector of the target epoch for secondary classification performed using linear discriminant analysis. The probabilities of belonging of an epoch to a certain class were estimated from the results of secondary classification.

The features used for the primary classification and the probabilities estimated after the secondary classification were used for the binary REMS/REMS classification with the XGBoost, where REMS is any class other than REMS (i.e., WP, LS, or DS). The end of the cycle was then identified using the following rule: "The cycle end is the end of a REMS epoch if at least five out of eight epochs to the left of it are REMS epochs and ten epochs to the right of it are non-REMS epochs."

After the recording was split into cycles, each epoch was marked with its normalized index in the cycle and the cycle number. These numbers were used to estimate a priori probabilities of belonging of an epoch to a certain class with the use of a mathematical model (a system of logistic regression equations). Let $P_m = \{p_w, p_r, p_l, p_d\}$ be a priori probabilities of belonging of an epoch to classes $\{w, r, l, d\}$, where w is WP, r is REMS, l is LS, and d is DS. These probabilities are estimated using the following model:

$$\begin{cases} p_w = \dfrac{1}{1+\exp(-y_w)}, \\ p_l = \dfrac{1}{1+\exp(-y_l)}, \\ p_d = \dfrac{1}{1+\exp(-y_d)}, \\ p_r = \dfrac{1}{1+\exp(-y_r)}. \end{cases}$$

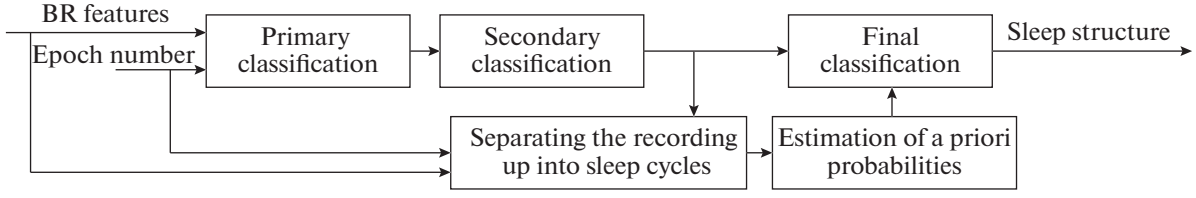

Fig. 6. Block diagram of the classification algorithm.

Table 1. Confusion matrix

Class determined by a physician on the basis of the PSG	Class determined by the algorithm from the BR data				
	WP	REMS	LS	DS	Sum
WP	M_{11}	M_{11}	M_{11}	M_{11}	R_1
REMS	M_{11}	M_{11}	M_{11}	M_{11}	R_2
LS	M_{11}	M_{11}	M_{11}	M_{11}	R_3
DS	M_{11}	M_{11}	M_{11}	M_{11}	R_4
Sum	C_1	C_2	C_3	C_4	N

Since the first and the last cycle are expected to differ from inner cycles, we write the following for y_i, $i \in \{w, r, l, d\}$:

$$y_i = \begin{cases} \beta_0 + \beta_1 t^3 + \beta_2 t^2 + \beta_3 t, & c = 1, \\ \beta_0 + \beta_1 t^3 + \beta_2 t^2 + \beta_3 t + \beta_4 c, & 1 < c < N, \\ \beta_0 + \beta_1 t^3 + \beta_2 t^2 + \beta_3 t, & c = N, \end{cases}$$

where t is the standardized epoch number in the cycle (1,...,100), c is the cycle number, and N is the total number of cycles in the recording.

The a priori probabilities need to be normalized, since their sum should not exceed unity:

$$p_i = \frac{p_i}{\sum\limits_{i \in \{w,l,d,r\}} p_i}.$$

Coefficients β were calculated based on the data of the SHHS sample (see above). If it was not possible to separate the recording into cycles, a priori probabilities $\{p_w, p_r, p_l, p_d\}$ were assumed to be constant and equal to {0.29, 0.15, 0.42, 0.14} for each epoch. These numbers represent the frequency of occurrence of the corresponding classes.

Final classification was performed using a neural network with one hidden layer of four neurons. Each epoch at the input was characterized by eight features: four probabilities estimated at the secondary classification stage and four a priori probabilities estimated using the above model.

E. Technique for Testing the Developed Algorithms and Methods

The artifact intervals and the RC peaks, which served as true answers in the process of testing the artifact and the RC identification algorithm, were marked manually in 27 BR recordings. The RCs were identified by means of visual analysis of synchronized BR and RIP signals. The average values of the sensitivity, specificity, and accuracy were calculated for the artifact identification by the algorithm. The average values of the sensitivity and accuracy were calculated for the RC identification by the algorithm.

The algorithm for determination of the sleep structure was tested by means of cross-validation for individual tested subjects. The training set was formed from features of 31 tested subjects, and the data for the remaining tested subject were used for testing. This procedure was repeated 32 times; the validation dataset (i.e., the number of the tested subject left out of the training set) was changed each time. At each iteration, the value of κ (Cohen's kappa) was calculated. The Cohen's kappa is a measure of the inter-expert agreement. In the case under consideration, the physician who determines the true classes of epochs is the first expert, and the algorithm is the second one. The Cohen's kappa is calculated as

$$\kappa = \frac{p_o - p_e}{1 - p_e},$$

where

$$p_e = \frac{\sum\limits_{i=1}^{n} C_i R_i}{N^2}$$

is the expected probability of chance agreement, and

$$p_o = \frac{\sum\limits_{i=1}^{n} M_{ii}}{N}$$

is the observed agreement among the experts.

Table 1 presents the confusion matrix for the problem of determination of the sleep structure. This is the matrix of correspondences between true sleep classes determined by a physician on the basis of the PSG data and the classes determined by the algorithm. Here, M_{ij} is the matrix element at the intersection of row i and column j, which represents the number of objects of class i assigned to class j by the the expert; R_i is the sum of the elements of row i; C_j is the sum of the elements of column j; and N is the total number of objects.

The Cohen's kappa may vary from −1 to 1. In the case of perfect agreement, $\kappa = 1$; if there is no agreement other than what would be expected by chance, $\kappa \le 0$.

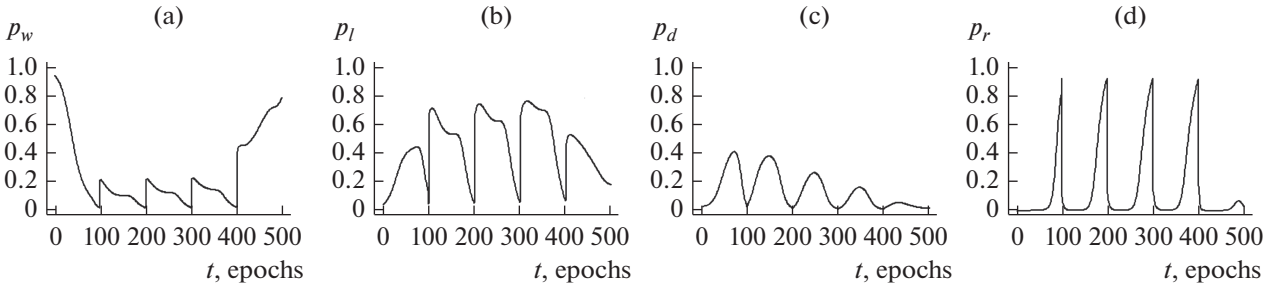

Fig. 7. Distribution of a priori probabilities (according to the model) for five sleep cycles of 100 epochs each: (a) wakefulness, (b) light sleep, (c) deep sleep, and (d) rapid eye movement sleep.

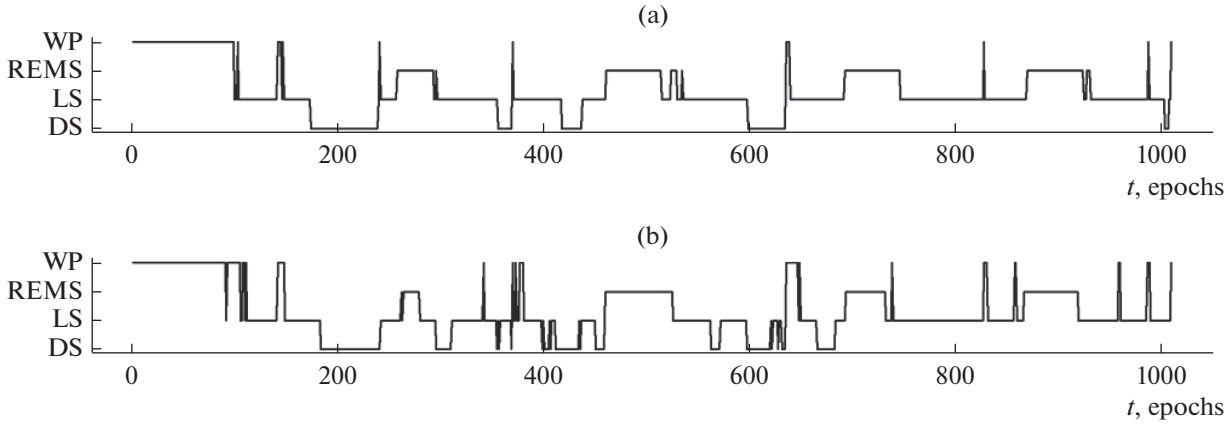

Fig. 8. Comparison of hypnograms of a tested subject without insomnia plotted by (a) a physician on the basis of the PSG data and (b) with the use of the algorithm based on the BR monitoring.

2. RESULTS

The average values of the sensitivity, specificity, and accuracy in the problem of determination of the sleep structure were 90%. The average values of the accuracy and sensitivity of RC identification were 96 and 98%, respectively.

The results of estimation of a priori probabilities with the use of the developed mathematical model for five sleep cycles of 100 epochs each are presented in Fig. 7.

The average quality of determination of the sleep structure was 0.5 Cohen's kappa for both insomniacs and apparently healthy test subjects. The quality of determination of the sleep structure for the entire sample was 0.50 ± 0.11 (mean $\pm$ standard deviation). Figures 8 and 9 show the hypnograms of tested subjects with and without insomnia. These hypnograms were plotted by a physician based on the PSG data and by the algorithm based on noncontact BR monitoring.

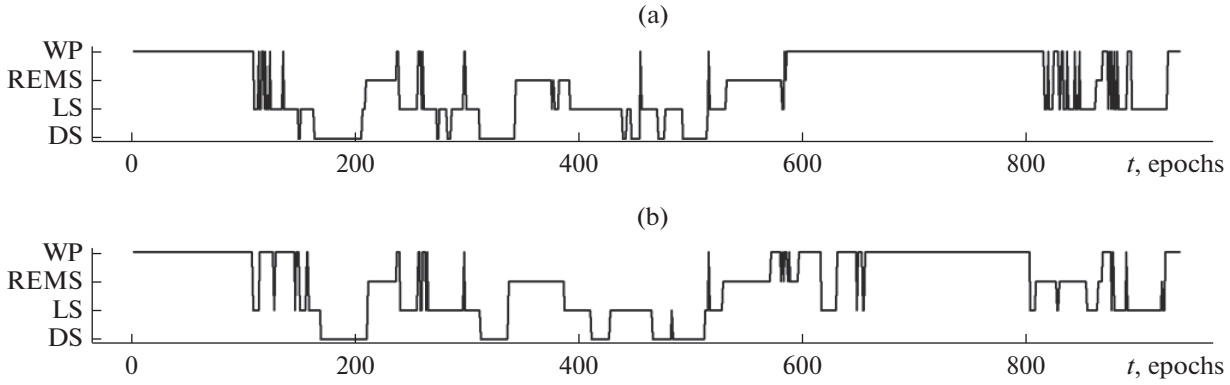

Fig. 9. Comparison of hypnograms of a tested subject with insomnia plotted by (a) a physician on the basis of the PSG data and (b) with the use of the algorithm based on the BR monitoring.

Table 2. Comparison of the results

Parameters of the study	Literature data					This study
	[4]	[14]	[15]	[16]	[17]	
Signals	RIP	ECG, RIP	RIP	BR	EEG, PSG	BR
Number of tested subjects	48	48	48	40	26	32
Number of features	26	80	27	–	–	23
Cohen's kappa	0.38 ± 0.14	0.49 ± 0.13	0.41 ± 0.17	0.47	0.61 (EEG) 0.74 (PSG)	0.50 ± 0.11

The results of comparison of the obtained data with the literature data are presented in Table 2.

3. DISCUSSION

The relatively low quality of artifact identification is attributed to the fact that, instead of establishing the presence of artifacts, we tried to determine whether a certain signal sample belongs to an artifact interval or not. Consequently, the quality indicators are affected negatively if an artifact is identified correctly but the boundaries of an artifact interval determined by the algorithm and the expert do not match perfectly.

The specificity for RC identification was not evaluated due to the fact that a true negative class (non-RC) is absent in this case. The indicators of the RC identification quality agree with the values obtained in other studies. For example, the authors of [18] reported a sensitivity of 97% in the RC identification in respiratory signals from a neonatal incubator, and a sensitivity of 94% was demonstrated in [19] in the RC identification in respiratory signals of sheeps recorded during hemorrhage.

The quality achieved by the developed algorithm for determination of the sleep structure based on the BR monitoring is higher than the values that were reported by other research groups and were obtained by analyzing cardiorespiratory features (including those recorded using standard contact techniques). However, the performance of this algorithm was validated only for apparently healthy tested subjects and a small group of insomniacs. Determining the applicability of the BR monitoring for the analysis of the sleep structure of subjects with sleep disorders and other diseases that may alter considerably the BR signal pattern requires additional investigations.

CONCLUSIONS

The results of automatic determination of the sleep structure based on the non-contact BR monitoring have been presented. The Cohen's kappa was 0.5 compared to the PSG results on calassification into four 2 classes of sleep epochs: WP, REMS, LS, and DS. The obtained result compares well with the results reported in the literature on determination of the sleep structure based on the cardiorespiratory analysis. Thus, the BR method may be used for long-term non-contact monitoring of the sleep structure.

ACKNOWLEDGMENTS

This study was supported by the Russian foundation for basic research (project nos. 15-07-02472 A and 16-07-01096 A).

REFERENCES

1. *Bioradar*, Ed. by A. S. Bugaev, S. I. Ivashov, and I. Ya. Imoreev (Izd. MGTU, Moscow, 2010) [in Russian].
2. *Principles and Practice of Sleep Medicine*, Ed. by M. Kryger, T. Roth, and W. C. Dement (Elsevier, Philadelphia, 2017).
3. I. S. Breslav, *Breathing Patterns: Physiology, Extremal States, Pathology* (Nauka, Leningrad, 1984) [in Russian].
4. X. Long, J. Foussier, P. Fonseca, et al., Biomed. Signal Proces. Control **14**, 197 (2014).
5. A. Tataraidze, L. Korostovtseva, L. Anishchenko, et al., in *Proc. 38th Annual Int. Conf. IEEE Medicine Biology Soc. (EMBC), Orlando, Aug. 16–20, 2016* (IEEE, New York, 2016), p. 2839.
6. A. Tataraidze, L. Korostovtseva, L. Anishchenko, et al., in *Proc. 38th Annual Int. Conf. IEEE Medicine Biology Soc. (EMBC), Orlando, Aug. 16–20, 2016* (IEEE, New York, 2016). p. 3478.
7. A. B. Tataraidze, L. N. Anishchenko, L. S. Korostovtseva, et al., Biomedits. Radioelektron., No. 7, 85 (2015).
8. S. Redline, M. H. Sanders, B. K. Lind, et al., Sleep **21**, 759 (1998).
9. D. A. Dean, A. L. Goldberger, R. Mueller, et al., Sleep **39**, 1151 (2016).

10. S. F. Quan, B. V. Howard, C. Iber, et al., Sleep **20**, 1077 (1997).
11. X. Long, P. Fonseca, J. Foussier, et al., IEEE J. Biomed. Health Inform. **18**, 1272 (2014).
12. S. J. Redmond and C. Heneghan, IEEE Trans. Biomed. Engineering **53**, 485 (2006).
13. T. Chen and C. Guestrin, in *Proc. 22nd ACM SIGKDD Int. Conf. Knowledge, Discovery and Data Mining (KDD 2016), San Francisco, Aug. 13–17, 2016* (Assoc. Comput. Machinery (ACM), New York, 2016).
14. P. Fonseca, X. Long, M. Radha, et al., Physiolog. Meas. **36**, 2027 (2015).
15. X. Long, J. Yang, T. Weysen, et al., Physiolog. Meas. **35**, 2529 (2014).
16. A. Zaffaroni, L. Gahan, L. Collins, et al., in *Proc. 22nd Congress Eur. Sleep Research Soc. (ESRS), Basel, Sept. 16–20, 2014* (ESRS, Basel, 2014).
17. J. R. Shambroom, S. E. Fabregas, and J. Johnstone, J. Sleep Research **21**, 221 (2012).
18. X. Navarro, F. Poree, A. Beuchee, and G. Carrault, Biomed. Signal Processing Control **16**, 9 (2015).
19. C. Daluwatte, C. G. Scully, G. C. Kramer, and D. G. Strauss, in *Proc. 2015 Computing in Cardiology Conf. (CinC), Nice, Sept. 6–9, 2015* (IEEE, New York, 2015).

Translated by D. Safin

SPELL: 1. wwere, 2. calassification